INTERNATIONAL JOURNAL OF HYDROGEN ENERGY 39 (2014) 1897–1902

Available online at www.sciencedirect.com

ScienceDirect

journal homepage: www.elsevier.com/locate/he

Stress-dependent hardening-to-softening transition of hydrogen effects in nanoindentation of a linepipe steel

Dong-Hyun Lee [a], Jung-A Lee [a], Moo-Young Seok [a], Un Bong Baek [b], Seung Hoon Nahm [b], Jae-il Jang [a,*]

[a] Division of Materials Science and Engineering, Hanyang University, Seoul 133-791, South Korea
[b] Division of Industrial Metrology, Korea Research Institute of Standards and Science, Daejeon 305-340, South Korea

ARTICLE INFO

Article history:
Received 16 July 2013
Received in revised form
11 October 2013
Accepted 15 November 2013
Available online 18 December 2013

Keywords:
Hydrogen
Nanoindentation
Hardness
Linepipe steel

ABSTRACT

We explored the influences of hydrogen on small-scale strength of a linepipe steel through nanoindentation experiments with four pyramidal indenters. Interestingly, a transition from hydrogen-induced hardening to softening was observed as indenter sharpness increases. The transition was analyzed based on the enhancement in hydrogen's elastic shielding effects for a sharper indenter, which could be indirectly evidenced by the stress effects on indentation pile-up, dislocation density, and rate dependency of hardness.

1. Introduction

Recently, the influence of hydrogen on the mechanical behavior of linepipe steels has gathered much research interests [1–5]. The motivations are two-fold. First, natural gas transmission pipelines can be exposed to hydrogen atmosphere (especially in the sour environment) [1,2,4]; i.e., hydrogen can be absorbed either from hydrogen sulfide (H_2S) included in natural gas or from localized corrosion and cathodic protection (in the buried pipeline). Second, such hydrogen research may be required for preparing the upcoming era of "hydrogen economy". It has been reported that, transporting gaseous hydrogen (in a form of either pure hydrogen or a blend of natural gas and hydrogen) through the existing natural gas pipelines may be the most cost-effective and energy-efficient way to transport large amounts of hydrogen over long distance [3]. Thus, understanding of the hydrogen effects on the mechanical performance of linepipe steels is essential for ensuring the safety and integrity of the hydrogen pipeline system.

Although it is well accepted that sufficient hydrogen deteriorates ductility and toughness in a linepipe steel [4,5] (which is often termed as hydrogen embrittlement [6]), there are contradictory aspects in the hydrogen effects on the plastic flow and dislocation mobility in a steel [6,7]; that is, sometimes hydrogen induces hardening [8,9] and sometimes softening [10,11], depending on the materials, hydrogen

* Corresponding author.
E-mail address: jijang@hanyang.ac.kr (J.-i. Jang).
0360-3199/$ – see front matter
http://dx.doi.org/10.1016/j.ijhydene.2013.11.060

concentration, and temperature [6,7]. For example, in austenitic stainless steels, many articles reported the hydrogen-induced increase in macroscopic yield strength [8,9], whereas hydrogen-induced decrease in microscopic strength was also observed through in-situ transmission electron microscopy observation [12] or internal friction measurement [13]. Matsui et al. [10] also reported that both H-induced hardening and softening can occur in high purity iron at low temperatures (170–300 K).

On the other hand, nanoindentation tests have been extensively performed for evaluating the hydrogen (H)-induced change in local mechanical properties [14–16] since they have strong advantage in addition to simple and easy procedure; i.e., nanoindentation tests require only small volumes of test material, making it possible to obtain statistically meaningful data from an identical sample. It is noteworthy that most of the nanoindentation studies to date have reported H-induced hardening [14–16] (that are explained by general solid solution hardening mechanisms such as dislocation dragging or pinning [16] and H-enhanced slip planarity [15]), but almost no nanoindentation research has been performed on the H-induced softening.

Plastic deformation mechanisms of metallic materials are known to be strongly dependent on the level of applied stresses and plastic strains, which can be also true for the H-affected deformation in hydrogenated samples. In this regard, it is somewhat interesting to note that (to the best of our knowledge) almost no efforts have been made on the issue. This is mainly due to the difficulty in changing stresses during nanoindentation tests with a typically-used three-sided pyramidal indenter (such as Berkovich indenter); i.e., from a continuum plasticity concept, the stresses and strains underneath a sharp indenter are unique and independent of indentation load or displacement due to the so-called geometrical self-similarity of the tip. This difficulty may be overcome by varying the sharpness of the pyramidal indenter which is characterized by its centerline-to-face angle, ψ. Generally, sharper indenters induce larger stresses and strains in the material due to the larger volume of material that is displaced [17–20]. Thus, indentations made with different ψ lead to different level of stresses and plastic strains, allowing a systematic evaluation of the effects of the imposed stresses and strains.

In this work, we systematically analyzed the influence of external stresses and plastic strains on the H-induced change in small-scale strength through a series of nanoindentation experiments with four triangular pyramidal indenters having different ψ from 35.3° to 75°. The purpose of this letter is to analyze our interesting observations that, with increasing the indentation stresses and strains, there is a clear transition from H-induced hardening to H-induced softening.

2. Experimental

The material under investigation was a commercial grade API X70 steel, one of the most popular natural gas pipeline steel, whose nominal chemical composition (in wt.%) is 0.071C–0.25Si–1.55Mn–0.25Cu–0.2Ni–0.04Nb–0.03V–0.015-Ti–0.03Al and (balance) Fe. The microstructure of the steel mainly consists of ferrite with very small fraction of pearlite. Surfaces of the specimens were ground with 2000-grit SiC paper and then electrolytically polished at 40 V for 60 s in a solution of 80% Ethanol, 14% distilled water, and 6% perchloric acid (according to ASTM E1558-09) in order to remove any hardened surface layer produced during grinding.

Electrochemical hydrogen charging was performed at room temperature with a potentiostat (HA-151A, Hokuto Denko, Tokyo, Japan) using a 0.25 g/L As_2O_3 in a 1 N H_2SO_4

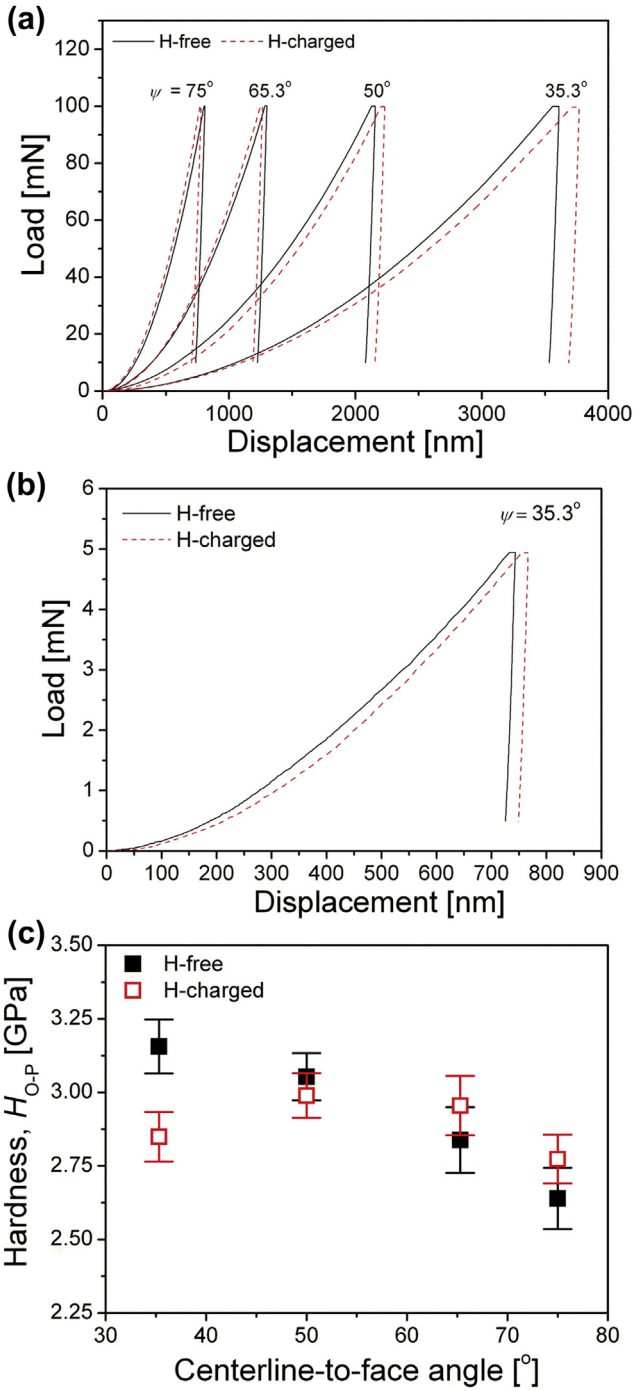

Fig. 1 – Influence of indenter angle on the nanoindentation results (obtained under an indentation strain rate of 0.05/s); (a) typical load-displacement curves conducted at P_{max} = 100 mN with various indenters; (b) the curves for ψ = 35.3° and P_{max} = 5 mN; (c) nanoindentation hardness.

solution. The As_2O_3 was added for enhancing the hydrogen atoms permeation and avoiding their recombination. While platinum and the specimen were used as anode and cathode respectively, hydrogen was charged into the specimen (having surface area of 1.1 cm^2) for 24 h under a constant current density of 100 mA/cm^2.

Nanoindentation tests were performed using a Nanoindenter-XP (formerly MTS now Agilent, Oak Ridge, TN) with four different triangular pyramidal indenters having a centerline-to-face angle ψ of 35.3° (cube-corner indenter), 50°, 65.3° (Berkovich indenter), 75°. The sample is loaded to the maximum load, P_{max}, of 100 mN at a constant strain rate, $(dP/dt)/P$ of 0.05/s. Since the steel samples desorb hydrogen with time after removal from solution, nanoindentation tests on the H-charged specimen were started within 30 min after hydrogen charging. More than 30 tests were performed for each condition. Hardness impression morphologies were imaged using a field-emission scanning electron microscopy (SEM), JSM-6330F (JEOL Ltd., Tokyo, Japan), and an atomic force microscopy (AFM), XE-100 (Park System, Suwon, Korea).

3. Results and discussion

Fig. 1(a) shows representative load-displacement (P–h) curves from nanoindentation experiments performed at the peak load of 100 mN with four different indenters. It is clear that the displacement at the peak load increases with decreasing ψ and, more importantly, H-charging significantly influences the elastoplastic (loading) part of the P–h curves. For clarity, the curves from cube-corner indentation made at low load (5 mN) are separately shown in Fig. 1 (b). The nanoindentation hardness values were estimated from the P–h curves according to the Oliver–Pharr method [21]. The area function (which is essential to calculate the hardness) for each indenter was determined through preliminary tests made on fused quartz. Fig. 1(c) summarizes the estimated hardness as a function of ψ. Somewhat surprisingly, the way in which the H-charging influences the hardness is strongly dependent on ψ; hardness of the hydrogenated sample is enhanced for less sharp indenters ($\psi = 65.3°$ and 75°), but is reduced for sharper indenters ($\psi = 35.3°$ and 50°). Especially, H-induced hardness decrease becomes more pronounced for $\psi = 35.3°$ than for 50°. This implies that there is a transition from H-induced hardening to H-induced softening with reduction in ψ. One may imagine that this transition is conceivably an artifact arising from the uncertainty about the applicability of the Oliver–Pharr method to various ψ. In the Oliver–Pharr method [21], the correlation constant β (that relates stiffness S to contact area A) is important for determining the area function and thus the hardness. However, the proper β is known only for the popularly-used Berkovich indenter (as a constant of 1.034), and the dependency of the β value on ψ is still unclear although some efforts have been made [22]. This may lead to miscalculations of the hardness data for other indenters used in this study.

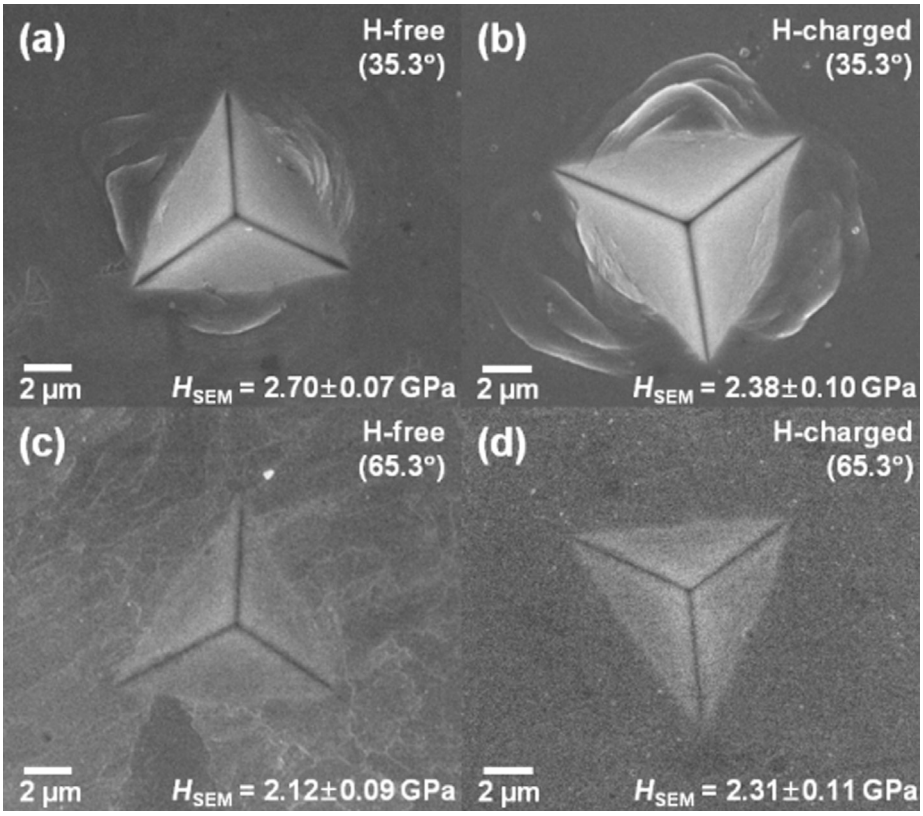

Fig. 2 – Representative SEM micrographs of nanoindentation impression for $\psi = 35.3°$ [(a), (b)] and $\psi = 65.3°$[(c), (d)]; (a), (c) are from H-free samples and (b), (d) are from H-charged ones. Adopted indentation strain rate was 0.05/s. Note that the magnification of each image is not exactly the same.

In order to check whether or not the hardening-to-softening transition in Fig. 1(c) is an artifact, the area of impression A was directly measured from a large number of SEM images for $\psi = 35.3°$ (cube-corner) and 65.3° (Berkovich), as shown in Fig. 2. Then, the hardness based on SEM images was calculated (as $P/A = 4P/(3\sqrt{3}a^2)$, where a is the averaged length measured from the center of the triangular impression to the corner) and listed in the images of Fig. 2. The H-charging indeed induces hardening for $\psi = 65.3°$, but softening for $\psi = 35.3°$, which supports that the intriguing hardening-to-softening transition with reducing ψ in Fig. 1(c) is realistic. Note that the hardness based on the SEM images (Fig. 2) are smaller than that according to Oliver–Pharr method because the material pile-up around indentation (shown in Fig. 2) is not taken into consideration in the Oliver–Pharr method and thus can induce an overestimated hardness [23,24].

As mentioned earlier, while the increase in nanoindentation hardness (H-induced hardening) is well known to be attributed to solid solution hardening (such as dislocation dragging or pinning) [16] or decreased ability of dislocations to cross slip [14,15], few nanoindentation research has reported the H-induced softening. In previous studies on the softening (mostly made through Vickers hardness tests [25] and/or uniaxial tensile tests [11]), two possible mechanisms have been suggested; one is increased mobility of screw dislocations and the other is elastic shielding of dislocation–defect interactions. First of these, an increased dislocation mobility (i.e., hydrogen modifies the Peierls potential of screw dislocations, thereby increasing their mobility [10]), is known to be more appropriate for high purity metals (such as high purity Fe [10]). Therefore, in the present study, we have more focused on the second one, so-called hydrogen's elastic shielding effect [26], which is now one of the mechanisms generally used for explaining the H-enhanced localized plasticity (HELP). Generally plastic flow and strength in a metallic material are predominated by elastic interactions between dislocations and between dislocations and other crystalline defects (which can be obstacles to dislocation motion such as solute atoms, impurities, and precipitates). In a hydrogenated sample, these interactions can be effectively reduced because H atoms may shield (or weaken) the stress fields of dislocations [11,25], which results in an increased dislocation mobility under stress, as the slip barrier can be more easily overcome by thermal activation [26].

An indirect evidence for occurrence of the elastic shielding in the cases of H-induced softening (i.e. $\psi = 35.3°$ and 50°) could be obtained from indentation morphology observations. During indentation of metallic materials, some portion of the material removed from the indented volume can pile-up around the indentation. The pile-up is known to become more pronounced as the strain hardening exponent (n of a power-law hardening relation; e.g., $\sigma \propto \varepsilon^n$) decreases [23] (due to the deteriorated ability to accommodate nanoindentation-induced plastic deformation by surrounding materials [27]). If the elastic shielding behavior occurs, the intensity of dislocation–dislocation interactions is diminished and thus n must be decreased [11]. This indicates that, if elastic shielding effect becomes stronger, the increase in pile-up amount in hydrogenated sample vis-à-vis H-free sample can be more pronounced. To investigate the details of pile-up behavior, surface profiles of hardness impression were examined using AFM. The ratio of the pile-up height ($h_{\text{pile-up}}$ measured with AFM) to the maximum displacement ($h_{\max}$ obtained from P–h curves), $h_{\text{pile-up}}/h_{\max}$, is plotted as a function of ψ in Fig. 3 where representative AFM images for $\psi = 35.3°$ and 65.3° are also provided. While the pile-up ratio increases with decreasing ψ in both H-free and H-charged samples, the influence of H-charging on the pile-up ratio is significantly affected by ψ. For less sharp indenters, the influence of H-charging on the pile-up ratio is almost negligible ($\psi = 75°$) or even the ratio is a little decreased in H-charged sample ($\psi = 65.3°$). For sharper indenters ($\psi = 35.3°$ and 50°), however, hydrogen enhances the pile-up ratio, and the increasing amount becomes larger as indenter sharpness increases from $\psi = 50°$ to 35.3°. All this pile-up behavior indicates that elastic shielding effect may be predominant mechanism for the H-induced softening observed here and becomes more pronounced with reducing ψ.

Another important clue for better understanding of the hardening-to-softening transition is dislocation density. Theoretical work by Birnbaum and Sofronis [26] proposed that elastic shielding becomes more significant as average distance between dislocations decreases (i.e., as dislocation density increases). Recently, Tal-Gutelmacher et al. [25] experimentally argued that the shielding effect was more pronounced in highly pre-deformed (cold rolled) samples due to the increase in dislocation density by the pre-straining. The representative strain underneath a sharp indenter is only dependent on the indent angle and is independent of indentation depth due to its geometrically self similarity, and total dislocation density underneath the indenter can be seriously affected by ψ. On one hand, a sharper indenter (having smaller ψ) induces larger stresses and plastic strains and resultantly produces higher degree of strain hardening and thus larger number of statistically-stored dislocations (SSDs). On the other hand, during indentation, geometrically necessary dislocations (GNDs) are also introduced in the material in order to accommodate the shape of the indenter and the density of GND increases as angle of conical indenter decreases according to the relation suggested by Nix and Gao, $\rho_{\text{GND}} = (3/2bh)\cot^2\theta$ [28], where b is the Burgers vector and θ is

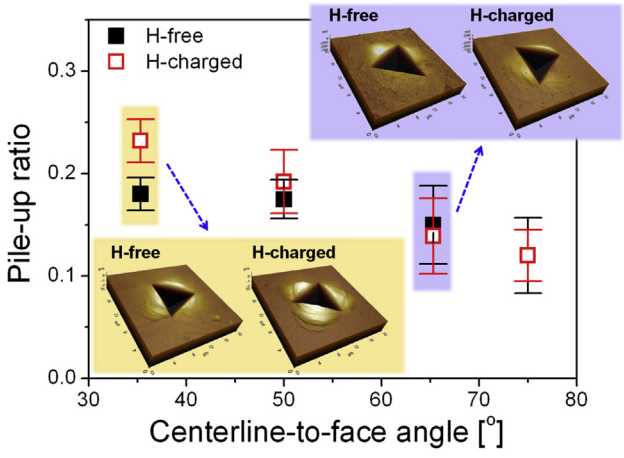

Fig. 3 – Variations in the pile-up ratio as a function of indenter angle.

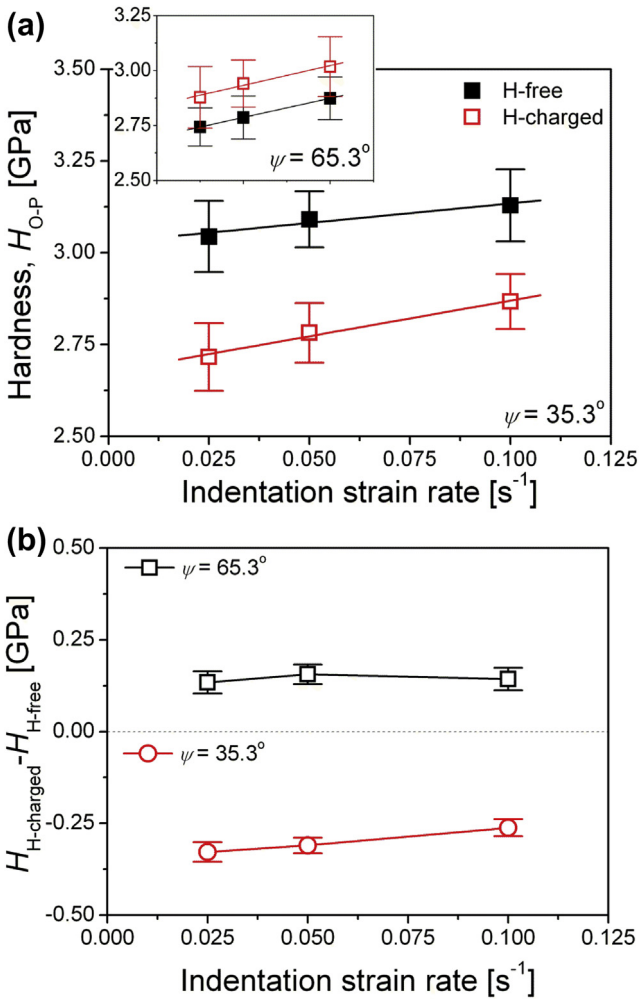

Fig. 4 – Influence of strain rate on (a) hardness and (b) the hardness difference between H-free and H-charged sample (for ψ = 35.3° and 65.3°).

the half-cone angle. The θ can be related to the ψ by $\theta = \tan^{-1}(\sqrt{3\sqrt{3}/\pi}\tan\psi)$ [29] which is derived under the assumption that similar behavior is obtained when the angle of the cone gives the same area-to-depth ratio as the pyramid. Thus, ψ values of 35.3°, 50°, 65.3° and 75° correspond to θ values of 42.3°, 56.9°, 70.3° and 78.2°, respectively. Therefore, total density of dislocations generated underneath the indenter increases with reducing ψ. Considering high mobility of H atoms even at room temperature [8], it is reasonable to believe that H interstitials diffuse quickly to the vicinity of indentation-generated SSDs and GNDs and forms H-environments around the new dislocations even upon loading sequence of nanoindentation test. This leads to a possibility that, if the indentation rate is increased, the shielding effect can be weakened due to insufficient time for H diffusion and hence for formation of H-environment around dislocations. The variations in hardness as function of indentation strain rate (for ψ = 35.3° and 65.3°) are summarized in Fig. 4(a), where hardness increases with strain rate in both H-free and H-charged samples. At a given strain rate, H-induced softening and hardening occur for ψ = 35.3° and 65.3°, respectively. To more clearly capture the influence of strain rate, the variations in hardness difference between H-free and H-charged sample ($H_{H\text{-charged}} - H_{H\text{-free}}$) with strain rate are also displayed in Fig. 4(b). For ψ = 35.3°, the extent of softening is reduced with increasing strain rate, which may indicate the decrease in density of the dislocations shielded by H-atmosphere. However, this scenario is based on elastic shielding theory and cannot hold valid for ψ = 65.3° showing H-induced hardening. For ψ = 65.3° in Fig. 4(b), hardness difference between H-free and H-charged sample is indeed almost independent of strain rate. Since Fig. 4(b) supports the possibility of the interactions between H interstitials and the newly-generated dislocations during nanoindentation, we could reach a conclusion that the hardening-to-softening transition with reducing ψ may be attributed to the increase in total dislocation density underneath the indenter and thus the enhancement in hydrogen's elastic shielding effect.

4. Conclusion

In the present study, hydrogen effects on deformation behavior of API X70 steel were investigated by nanoindentation experiments with four different triangular pyramidal indenters. Hardness of hydrogenated samples increases for less sharp indenters (ψ = 65.3° and 75°), but decreases for sharper indenter (ψ = 35.3° and 50°). The transition from H-induced hardening to softening with reducing ψ is analyzed based on the increase in hydrogen's elastic shielding effects for a sharper indenter, which can be indirectly evidenced by the effects of indentation stresses and strains on indentation pile-up behavior, density of dislocations generated underneath indenter, and strain-rate dependency of hardness.

Acknowledgment

This work was supported by the Korea Research Council of Fundamental Science and Technology (KRCF) through the National Agenda Project, and partly by the Human Resources Development program of the Korea Institute of Energy Technology Evaluation and Planning (KETEP) grant funded by the Korea Government Ministry of Trade, Industry and Energy (No. 20134030200360).

REFERENCES

[1] Park GT, Koh SU, Jung HG, Kim KY. Effect of microstructure on the hydrogen trapping efficiency and hydrogen induced cracking of linepipe steel. Corros Sci 2008;50:1865–71.
[2] Capelle J, Gilgert J, Dmytrakh I, Pluvinage G. Sensitivity of pipelines with steel API X52 to hydrogen embrittlement. Int J Hydrogen Energy 2008;33:7630–41.
[3] Gao M, Krishnamurthy R [chapter 10]. In: Gupta RB, editor. Hydrogen fuel: production, transport, and storage. New York: CRC Press; 2009.
[4] Hardie D, Charles EA, Lopez AH. Hydrogen embrittlement of high strength pipeline steels. Corros Sci 2006;48:4378–85.

[5] Lee J-A, Lee D-H, Seok M-Y, Baek UB, Lee YH, Nahm SH, et al. Hydrogen-induced toughness drop in weld coarse-grained heat-affected zones of linepipe steel. Mater Charater 2013;82:17–22.
[6] Hirth JP. Effects of hydrogen on the properties of iron and steel. Metall Mater Trans A 1980;11A:861–90.
[7] Murakami Y, Kanezaki T, Mine Y. Hydrogen effect against hydrogen embrittlement. Metall Mater Trans A 2010;41A:2548–62.
[8] Abraham DP, Altstetter CJ. The effect of hydrogen on the yield and flow stress of an austenitic stainless steel. Metall Mater Trans A 1995;26A:2849–58.
[9] Asano S, Otsuka R. The lattice hardening due to dissolved hydrogen in iron and steel. Scripta Metall 1976;10:1015–20.
[10] Matsui H, Kimura H, Moriya S. The effect of hydrogen on the mechanical properties of high purity iron. Mater Sci Eng 1979;40:207–16.
[11] Brass A-M, Chene J. Hydrogen uptake in 316L stainless steel: consequences on the tensile properties. Corros Sci 2006;48:3222–42.
[12] Rozenak P, Robertson IM, Birnbaum HK. HVEM studies of the effects of hydrogen on the deformation and fracture of AISI type 316 austenitic stainless steel. Acta Metall Mater 1990;38:2031–40.
[13] Gavriljuk VG, Shivanyuk VN. Diagnostic experimental results on the hydrogen embrittlement of austenitic steels. J Foct Acta Mater 2003;51:1293–305.
[14] Morasch KR, Bahr DF. The effects of hydrogen on deformation and cross slip in a BCC titanium alloy. Scripta Mater 2001;45:839–45.
[15] Nibur KA, Bahr DF, Somerday BP. Hydrogen effect on dislocation activity in austenitic stainless steel. Acta Mater 2006;54:2677–84.
[16] Barnoush A, Asgari M, Johnsen R. Resolving the hydrogen effect on dislocation nucleation and mobility by electrochemical nanoindentation. Scripta Mater 2012;66:414–7.
[17] Jang J-i, Lance MJ, Wen S, Tsui TY, Pharr GM. Indentation-induced phase transformations in silicon: influences of load, rate and indenter angle on the transformation behavior. Acta Mater 2005;53:1759–70.
[18] Jang J-i, Pharr GM. Influence of indenter angle on cracking in Si and Ge during nanoindentation. Acta Mater 2008;56:4458–69.
[19] Shim S, Jang J-i, Pharr GM. Extraction of flow properties of single-crystal silicon carbide by nanoindentation and finite-element simulation. Acta Mater 2008;56:3824–32.
[20] Jang J-i, Yoo B-G, Kim JY. Rate-dependent inhomogeneous-to-homogeneous transition of plastic flows during nanoindentation of bulk metallic glasses: fact or artifact? Appl Phys Lett 2007;90:211906.
[21] Oliver WC, Pharr GM. An improved technique for determining hardness and elastic modulus using load and displacement sensing indentation experiments. J Mater Res 1992;7:1564–83.
[22] Strader JH, Shim S, Bei H, Oliver WC, Pharr GM. An experimental evaluation of the constant β relating the contact stiffness to the contact area in nanoindentation. Philos Mag 2006;86:5285–98.
[23] Bolshakov A, Pharr GM. Influences of pileup on the measurement of mechanical properties by load and depth sensing indentation techniques. J Mater Res 1998;13:1049–58.
[24] Lee YH, Hahn JH, Nahm SH, Jang JI, Kwon D. Investigations on indentation size effects using a pile-up corrected hardness. J Phys D Appl Phys 2008;41:074027.
[25] Tal-Gutelmacher E, Eliezer D, Boellinghaus T. Investigation of hydrogen-deformation interactions in β-21S titanium alloy using thermal desorption spectroscopy. J Alloys Comp 2007;440:204–9.
[26] Birnbaum HK, Sofronis P. Hydrogen-enhanced localized plasticity-a mechanism for hydrogen-related fracture. Mater Sci Eng A 1994;176:191–202.
[27] Barnoush A. Correlation between dislocation density and nanomechanical response during nanoindentation. Acta Mater 2012;60:1268–77.
[28] Nix WD, Gao H. Indentation size effects in crystalline materials: a law for strain gradient plasticity. J Mech Phys Solids 1998;46:411–25.
[29] Jang J-i, Yoo B-G, Kim Y-J, Oh J-H, Choi I-C, Bei H. Indentation size effect in bulk metallic glass. Scripta Mater 2011;64:753–6.